Measuring the Effect of Moist Droplet-laden Flow on Transonic Compressor Cascade Performance

Silvio Geist, Niklas Neupert, Franz Joos

Measuring the Effect of Moist Droplet-laden Flow on Transonic Compressor Cascade Performance

Silvio Geist[1]*, Niklas Neupert[2],Franz Joos[3]

ISROMAC 2017

International Symposium on Transport Phenomena and Dynamics of Rotating Machinery

Maui, Hawaii

December 16-21, 2017

Abstract

This study provides insight on the influence of air humidity on droplet laden flow as it occurs during inlet fogging and in steam turbines. 2D-LDA is used to gather air-only data at three different humidities to rate humidity-depended cascade losses such as shock and profile boundary layer losses. Likewise, change in aerodynamics is explained using a combination of isentropic and Rayleigh flow. Then, water droplets are added to the flow field and data is collected using 2D-PDA. Again losses are evaluated.

Regarding the droplet-free flow, effects and relations found in literature could be confirmed for the presented cascade flow. However, the results further indicate that for droplet-laden flows favourable humidity effects are decreased and may be neglected since the major loss arises from the increased boundary layer thickness.

Keywords

thermodynamics of two-phase flows — air-humidity — shock wave — condensation — evaporation

[1,2,3] *Laboratory of Turbomachinery, Helmut-Schmidt-University / University of the Federal Armed Forces, Hamburg, Germany*

*__Corresponding author__: silvio.geist@hsu-hh.de

NOMENCLATURE

variables

D_{10}	droplet mean diameter
D_{32}	droplet Sauter mean diameter
Ma	isentropic Mach number
T_{tot}	total temperature
T	temperature
X_L	air's specific humidity
R	air's individual gas constant
c	chord length
c_p	air's heat capacity at constant pressure
t	passage height
$w_{1/2}$	velocity at traverse one and two
$\beta_{1/2}$	flow angle at at traverse one and two
$\delta\theta$	incremental wake height
κ	heat capacity ratio
Θ_w	momentum displacement thickness
Θ_{99}	boundary layer thickness
ω_{loss}	loss coefficient
ξ_m	droplet mass fraction

INTRODUCTION

Nowadays, power demands are met by an increasing amount of renewable resources. However, peak loads are still covered by conventional approaches such as gas turbines which have to respond quickly on possible supply fluctuations of the renewables. In that regard, high-fogging is a common procedure to enhance gas turbine power output. Small-sized water droplets, sprayed into the engine's inlet, are intended to evaporate, thus absorbing heat from the surrounding flow. As a result the specific work needed for compression is reduced. For instance this increase in flexibility helped to fulfill the stringent requirements of the UK grid code by providing an additional extra output of 18 MW for the Marchwood power plant within a short period of time [1].

Apparently, high-fogging is particularly useful in hot regions where the cooling potential is high. Regarding, e.g. equatorial areas, operating conditions may not only be hot, but also at a high level of humidity. Furthermore the procedure itself changes the air's humidity. As a result regions of different saturation occur within the flow field, giving rise to condensation.

Especially transonic flow fields, as they occur in the tip region of compressor blading, in turbine passages, nozzels and around airfoils may be altered strongly that way. Hence, understanding the interaction of the two opposing processes of evaporation and condensation is essential for realistic design of turbomachinery under atmospheric conditions. Schnerr and Dohrmann [2],[3] calculated transonic flow around an airfoil and found that increasing humidity decreases shock strength and shifts the shock position downstream. This is due to local condensation of water vapour. If moist air is accelerated along the airfoil's suction side, static pressure and temperature will decrease. That reduces the air's dew-point and encourages condensation. During condensation, heat is released into the surrounding gas, which decreases the local Mach number and eventually reduces shock intensity.

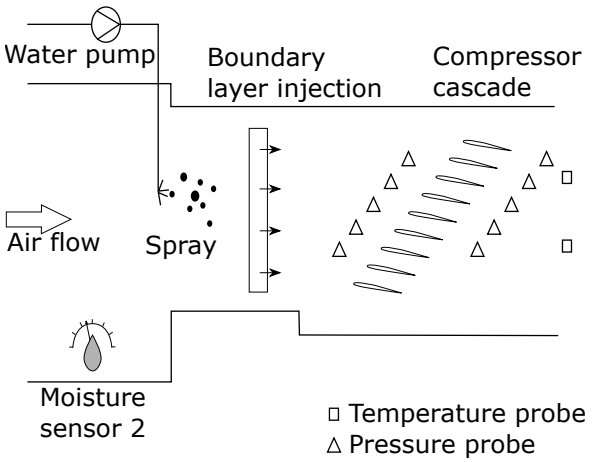

Figure 1. Illustration of the measurement section

More recently, Sasao and Yamamoto [4] conducted 2D calculations with dry and moist air through transonic compressor and turbine cascades alike. They validate their code against measured turbine cascade data gathered by Nagayama et al. [5] in 1982. Unfortunately, no reference measurement data were on hand for the transonic compressor case which underlines the need of the present study. Both measurements and simulation indicate increased total pressure losses in condensation cases, although shock strength and position remained almost unaltered. Concerning compressors, however, they state a rise in passage static pressure which drives the shock downstream and strengthens it.

Although moisture effects on transonic flow is studied thoroughly, the interaction of both moist and droplet-laden flow in the vicinity of shocks is not well understood. Hence, it is of great relevance for compressor power enhancement through fogging or wet steam turbine operation.

This study presents measurements of transonic compressor cascade flow velocity utilising a 2D-LDA/PDA system. Performance quantities deflection, velocity ratio and profile loss are used to evaluate the different flow conditions. Furthermore, to illustrate the underlying physics the throughflow is expressed as a combination of isentropic and Rayleigh flow.

1. METHODS

This section briefly presents the test rig's structure before mentioning measurement instruments used. That includes pressure and temperature probes to monitor operating point, moisture sensors to gain humidity information as well as a description of the optical 2D-LDA/PDA system. Then, the measurement campaign is outlined. Finally, this study's key performance parameter, loss coefficient, is introduced.

Test Rig To clarify the impact of droplets on moist flows and vice-versa nine blades with profiles similar to modern compressors' outer cross-sections have been mounted within a cascade as shown in Fig. 1. That creates a similar flow field, as it can be found in the tip regions of real gas turbine

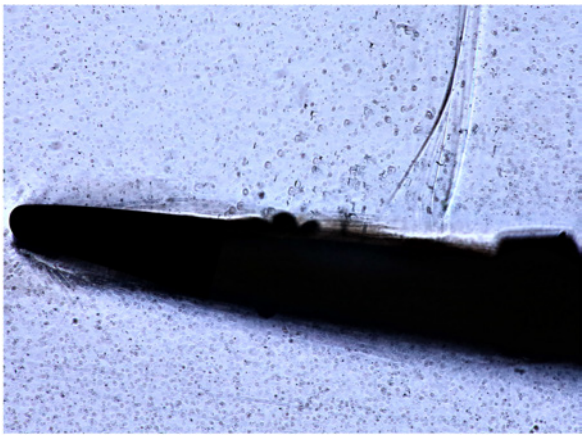

Figure 2. Schlieren photograph of air-only flow at $\beta_1 = 153°$ and $X_L = 3\,\mathrm{g/kg}$; clearly visible is the normal shock located at about one third of the total chord length

parameter	value
c	0.05 m
t	0.05 m
Ma_1	0.95
β_1	146°.. 154°
$T_{Tot,1}$	304 K

Table 1. Test rig parameters summary

compressor stages. Previous studies have shown a nearly undisturbed flow around the centre blades regarding the lower and upper test section walls. Hence, all measurements are conducted around the fourth and the fifth blade counting from the lower wall.

The accompanied wind tunnel is situated at the Laboratory of Turbomachinery at the Helmut-Schmidt-University in Hamburg, Germany. Outside air is compressed by a radial compressor which is then led into the test rig's settling chamber. Excess air may be bypassed to adjust mass flow precisely. The settling chamber is a boiler-shaped cylinder which is 1.6 m in diameter. Several sieves equalise flow before it is accelerated through a nozzle to enter the test section. Since, the inlet Mach number of $Ma_1 = 0.95$ is close to unity and increased compared to the design value of $Ma_{design} = 0.89$ a shock system is always existent on the blades' suction sides as displayed in Fig. 2. Outlet air is purged in a water-separator before it is discharged through the chimney.

Build-in variable vanes back pressure the flow to set a pressure ratio across the measurement section. Notable cross-section parameters are listed in Tab. 1 and illustrated in Fig. 3 for convenience. Further details of the test rig can be found in [6]. Note that the velocity triangle in Fig. 3 only underlines the substitution of the relative velocities $w_{1/2}$ through the cascades air flow. Hence, the cascade is not rotating or moving.

Instrumentation Overall, three air-only data sets at different specific humidities, namely $X_L = 3\,\mathrm{g/kg}$, $X_L = 6\,\mathrm{g/kg}$

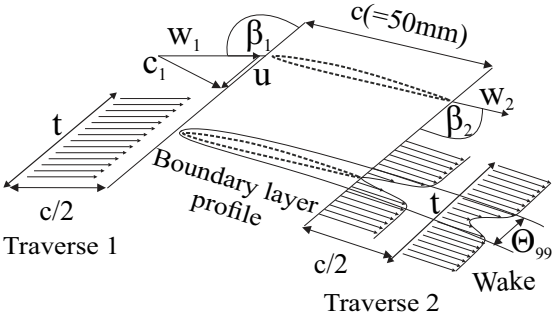

Figure 3. Illustration of cascade nomenclature

and $X_L = 11$ g/kg were measured at different blade loadings while the inlet Mach number and total temperature were kept constant. This is monitored using five pressure taps and two hard-wired resistance thermometers on each side wall. The inflow angle was set using a crank mechanism which rotates the cascade's blades around the centre blades leading edge. However, inflow angles used for calculation and evaluation were measured using the more precise 2D-LDA along traverse 1 in Fig 3.

To ensure a well defined specific humidity two moisture sensors have been utilised. The first measures the water content of the air drawn from the environment. Based on that measurement demineralised water is sprayed in the air supply's outlet to adjust moisture at the second sensor position in front of the cascade. Due to high duct temperature and residence time within the duct connecting the supply with the settling chamber the spray is evaporated entirely therein. To maintain a virtually 2D flow in the test section, the sidewall boundary is re-energised using compressed air which is injected via a slit nozzle system in front of the cascade [7].

In addition to the air-only measurements each parameter set was measured with a droplet mass fraction of $\xi_m = 0.01$. That is the ratio of droplet mass to total mass. To do so, water was injected into the settling chamber via a manifold of 10-15 impingement nozzles (BETE PJ10) generating a spray with a mean diameter $D_{10} = 7.0\,\mu$m and a Sauter mean diameter $D_{32} = 38.7\,\mu$m at the cascade's entrance equaling those utilised in industrial overfogging applications [8].

A non-invasive 2D-LDA/PDA technique was used to collect the flow field's velocity components. Sidewalls made of acrylic glass allow visual access. Light was supplied by a 5 W Argon-Ion laser. A 2D probe with a lens of 160 mm focal length and no beam expansion was used. That resulted in a measuring volume of 0.078 mm x 0.077 mm x 0.65 mm for the 514.5 nm beam and 0.074 mm x 0.073 mm x 0.62 mm for the 488 nm beam. To conduct both, LDA and PDA measurements with only one setup a side scatter configuration was chosen which included a fiberPDA photomultiplier and a Dantec BSA signal processor to process the photomultiplier output. The system is capable of measuring velocities with an error of less than 6 % and droplet diameters with less than 3 %. It was traversed half a chord length ($c = 50$ mm) in front of the blades leading edges to gather inlet information. After traversing through the passage the profiles wake was eventually measured at traverse 2, situated half a chord length downstream the trailing edge. Based on that data performance parameters, profile loss and isentropic Mach number distribution through the passage were extracted and evaluated.

To account for local temperature change while traversing through the passage the speed of sound is determined based on the measured local velocity and inlet total temperature which is measured within the settling chamber. Consequently, the general Mach number

$$Ma = \frac{w}{\sqrt{T\kappa R}} \tag{1}$$

is altered by substituting local temperature using

$$T_{tot} = T + \frac{w^2}{2c_p} \tag{2}$$

which eventually yields

$$Ma = \frac{w}{\sqrt{\left(T_{tot} - \frac{w^2}{2c_p}\right)\kappa R}} \tag{3}$$

as the local isentropic Mach number discussed herein.

Loss coefficient This parameter has been used in previous research [9] and is repeated here for convenience.

$$\omega_{loss} = \frac{2\,\Theta_w}{t\,cos\beta_2}\left(\frac{\overline{w_2}}{\overline{w_1}}\right)^2 \tag{4}$$

where

$$\Theta_w = \int_{\Theta_{99}} \left(1 - \frac{w_2}{\overline{w_2}}\right)\frac{w_2}{\overline{w_2}}\delta\Theta \tag{5}$$

is the wake momentum thickness. The loss coefficient is based on velocity measurements and is the only applicable source of information about the losses in the cascade since reliable measurements of total pressure were not possible due to droplet disturbance. Eqn. 4 consists of two main terms, mean deceleration over the cascade and the momentum wake losses accounted in Eqn. 5. Hence, traverse two velocity distributions with narrower wakes containing a high momentum, generate fewer losses than a comparable fast outflow with a broad wake. The question arises on which distance to measure such a wake. Scholz [10] states up to 20 % deviation when simply averaging outflow velocity and angle at an arbitrary downstream position. Therefore, he proposes a method to compute the equivalent homogeneous outflow where wake has vanished. Values $\overline{w_2}$ and β_2 used during loss computation have been computed according to that method. These terms will be of great importance later on. Due to the fact that ω_{loss} was derived by the integration of the wake, only the loss of momentum was accounted for.

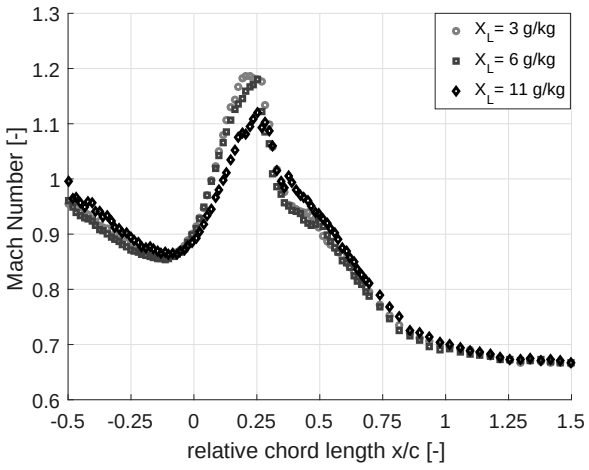

Figure 4. Isentropic Mach number over passage traverse at $\beta_1 = 154°$ for different humidities

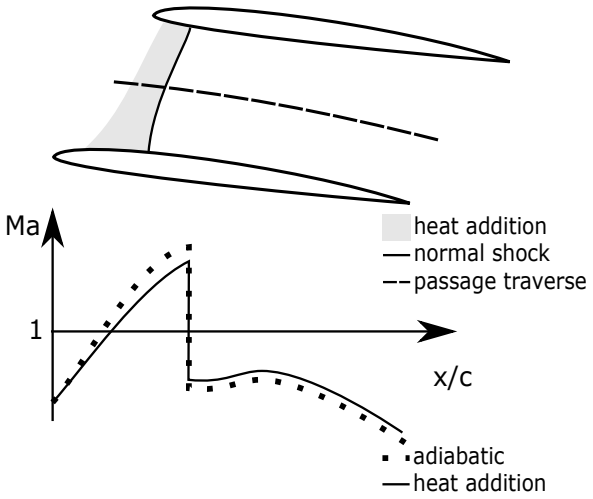

Figure 5. Top: Scheme of compressor blade passage Bottom: Mach number distribution at the dashed line for a combined isentropic /Rayleigh flow and pure isentropic flow with varying cross-section according to [12]

Thus, the evaluation of losses based on momentum deficit sufficed when droplets are added to the flow. However, only the smallest droplets ($< 2\,\mu m$) which followed the airflow closely were taken into account during the evaluation. Note that thermodynamic effects between the phases, such as heat transfer, were omitted when it came to loss analysis. In conclusion, this paper rates the aerodynamic losses due to heat transfer between the phases, but not the heat transfer loss itself. This might be a goal of future publication.

2. RESULTS AND DISCUSSION

The aim of this study is to provide information and insights on how compressor cascade's wake and shock losses change for air of different humidity in the vicinity of droplets. Thus, air-only measurements are first presented and evaluated. These results illustrate flow features as they are stated in the literature which verifies the over-all approach. Here, the change in state values is illustrated utilising a combination of isentropic and Rayleigh flow to explain underlying physics. Then, data including droplets are presented and compared to air-only flow to derive coupling effects between the substances. Finally, performance data are compared to rate the influence of humidity on both cases. Please note that these data originate from a greater campaign. For more measurement data, including different cross-sections, sprays and surface wetabilities be referred to [11].

2.1 Air-only results

First, differences in isentropic Mach number distribution due to humidity at a specific inflow angle are examined which eventually leads to a diabatic treatment of the flow. Second, humidity impact on the cascade performance is evaluated based one the loss coefficient ω_{loss} thus considering wake and profile boundary layer loss.

Diabatic Flow Fig. 4 displays the humidity depended distributions of local Mach number through the passage centre line. Before heading to the humidity dependence recall that compressor passage shape is very similar to a diffuser. Consequently, when flow is accelerated around the leading edge ($x/c = 0$) reaching supersonic conditions, as it is the case in that study, the diffuser shaped passage accelerates the flow even further ($0.25 > x/c > 0$) as in the divergent part of a Laval nozzle. When the shock delays flow into the subsonic region ($x/c > 0.25$) it is in turn slowed down by the divergent passage shape, forming the well known Mach number distribution. Now, comparing distributions at different humidity levels, it is apparent that an increased humidity lowers the pre shock Mach number and thus reduces shock strength. This behaviour may be expressed by a flow as proposed by Schneer [12] who researches stability of compressible fluids with energy supply. It holds the following conditions:

- flow is of converging diverging nozzle type
- one-dimensional flow
- variable cross-sectional area
- heat exchange.

Schnerr incorporates both Hugoniot equations for shock and Rayleigh equations for heat exchange treatment. That results in formulations describing state variable change through the passage which are extensions of the well known adiabatic shock solutions.
Figure 5 illustrates such an abstract Mach number distribution along the dashed line. The continuous heat addition through droplet condensation during supersonic flow conditions increases static pressure, thus reducing dynamic pressure, and local speed of sound. [12],[4] Both effects evoke a reduction of the maximum Mach number and the preceding Mach number slope. However, measurement data do not account for the temperature effect since Mach number is calculated based on inlet total temperature and no information

on field temperature is available.
Still, theory depicts measurements well, thus giving a meaningful aid when understanding the physical background. Keeping that in mind wake loss is examined over the inflow angle range within the next section.

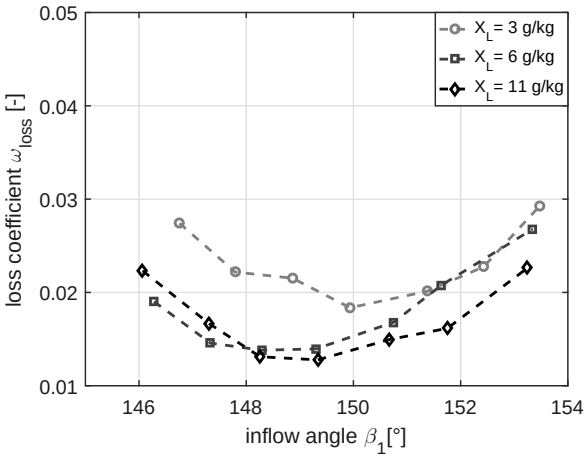

Figure 6. Loss coefficient for dry and humid air flow at various incidence angles

Loss coefficient Fig. 6 shows loss coefficient ω_{loss} for inflow angles ranging from β_1=146° to β_1= 154°.
Loss coefficient is highest at specific humidity $X_L = 3\,\mathrm{g/kg}$ over the entire range of measured data, whereas humidity in general reduces the loss coefficient. The reason for this are reduced shock losses due to the aforementioned theory. More precisely, regarding ω_{loss}, wake momentum thickness Θ_w is reduced through a decreased wake height as it is shown in Fig. 7. As for the loss curve, the overall trend is related to the altered blade loading and the, in this particular case more important, curve's offsets are induced by the change in humidity. At higher blade loadings , i.e. $\beta_1 > 149°$ an increase of specific humidity further decreases loss since wake heights Θ_w for $X_L = 6\,\mathrm{g/kg}$ and $X_L = 11\,\mathrm{g/kg}$ diverge with the latter having the smaller slope. Considering small inflow angles there is still a notable wake momentum thickness reduction when compared with dry flow. A further humidity increase has no significant effect. Yet, note the intersection at $\beta_1 = 148.5°$.
Surprisingly, focusing again on Fig. 6, $X_L = 6\,\mathrm{g/kg}$ depicts smaller loss for $\beta_1 < 149°$ and losses re-increase for $X_L = 11\,\mathrm{g/kg}$. The reason is the alteration of mean deceleration through humidity illustrated in Fig. 8.

For high blade loading the passage shock is situated near the leading edge which is why mean deceleration at the back traverse remains constant for all three humidity levels since curvature acceleration is large compared to the humidity effect. That is illustrated clearly for large inflow angles in Fig. 8. With decreasing inflow angle curves diverge and eventually characteristics of the intermediate and high humidity cross at $\beta_1 = 148.5°$. That indicates that mean back traverse

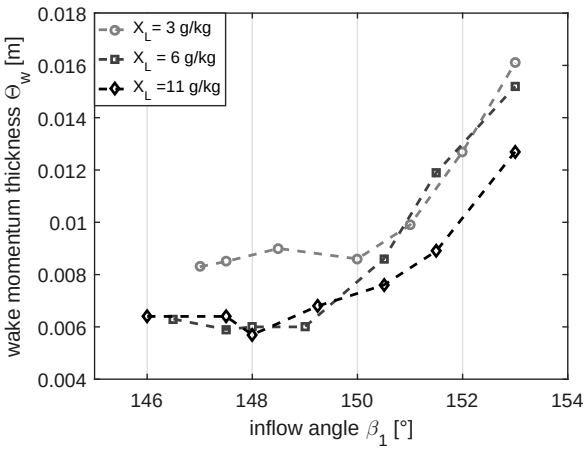

Figure 7. Wake momentum thickness Θ_w over inflow angle at different humidities

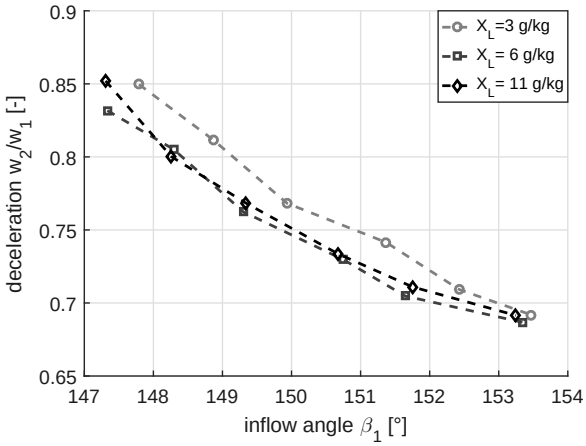

Figure 8. Deceleration w_2/w_1 of equivalent, homogeneous flow based on back traverse data over inflow angle at different humidities

velocity is notably greater in the latter case.
The main reason for this is that the passage shock moves towards the trailing edge for small inflow angles which alone strongly influences $\overline{w_2}$. Furthermore the condensation additionally pushes the shock downstream. Post-shock Mach number and thus back traverse velocity is much higher due to the reduced shock strength. That in turn decreases cascade performance. However, for high blade loadings shock position is located near the leading edge and $\overline{w_2}$ is nearly constant due to the curvature acc- and deceleration.

2.2 Droplet-laden results

This section discusses measurement results when droplets ($\xi_m = 0.01$) are present within the flow. It has to be noted at that point that the vicinity of droplets, i.e. the existence of a fluid phase changes flow properties such as density, compressibility and speed of sound as stated by Brennen [13]. He encourages to use so called effective values describing an equivalent homogeneous distributed gas. Such effective

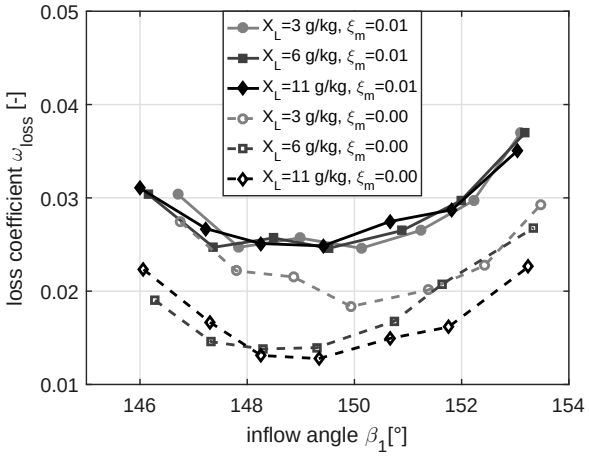

Figure 9. Comparison of loss coefficients for air-only and droplet-laden flow at various incidence angles

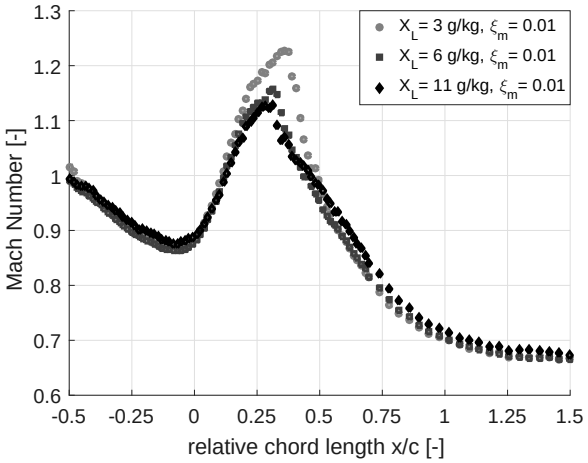

Figure 10. Isentropic Mach number over passage traverse $\beta_1 = 154°$

values are basically ideal gas values weighted with particle loading, i.e. ξ_m. As a consequence, for a droplet-laden flow with $\xi_m = 0.01$, effective Mach number is about 1.3 % higher compared to isentropic flow conditions. However, for a clear description of the humidity effect, droplet-laden results are still expressed using isentropic inflow Mach number.
According to theory those droplets act as heat sinks when evaporating on the one hand and on the other hand as condensation nuclei. Hence, a change in the net heating could be expected.

In fact, comparing the loss coefficients as displayed in Fig. 9 all wet flow curves not only generate more losses, but cluster as well. This is in distinct contrast to the air-only results. Especially, when consulting the Mach number through the passage shown in Fig. 10 which basically shows distributions as expected. First, a high specific humidity decreases the pre shock Mach number and shock strength. Second, droplets evaporate and cool the flow. This accelerates the flow resulting in an about 5 % higher peak Mach number of $Ma_1 \approx 1.25$ for $X_L = 3\,\mathrm{g/kg}$ compared to $Ma_1 \approx 1.2$ at air-only conditions. For humid air this cooling potential is reduced due to saturation limit, resulting in smaller slopes for cases $X_L = 6\,\mathrm{g/kg}$ and $X_L = 11\,\mathrm{g/kg}$. Consequently, that does not explain similar loss coefficients at different humidities. Regarding deflection a decrease between 5 % and 15 % can be stated which is similar to air-only flow. A quick view on the comparison of deceleration ratios in Fig. 11 excludes that term as the reason as well. No significant change between air-only and wet cases at constant humidity is recognisable. In fact the constant, high loss is caused by a thickened wake momentum thickness as shown in Fig. 12. That loss is dominant compared to the performance gain due to reduced shock loss.

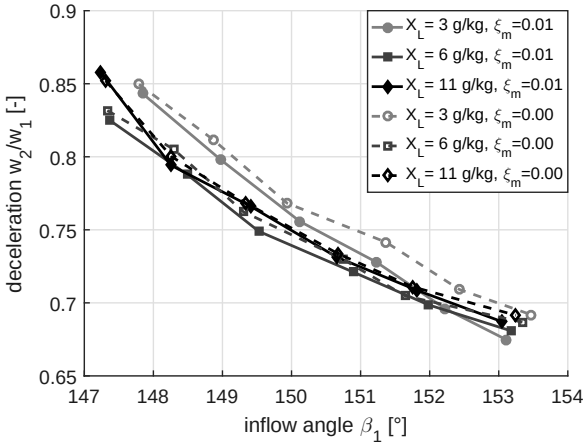

Figure 11. Comparison of deceleration w_2/w_1 of equivalent, homogeneous air-only and droplet-laden flow based on back traverse data over inflow angle at different humidities

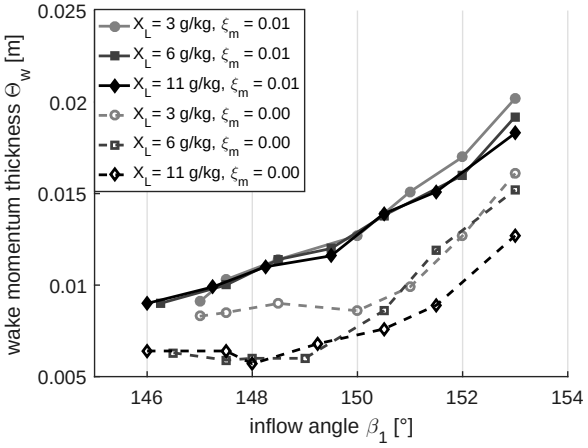

Figure 12. Comparison of wake momentum thickness Θ_w for air-only and droplet-laden flow over inflow angle at different humidities

2.3 Conclusions

As thermodynamic effects between the phases are neglected so far, the evaluation of losses based on momentum deficit

stays valid when droplets are added to the flow. That is why cascade losses do not account for the potential decrease of evaporation due to the simultaneous condensation at the moment. A study examining the combined performance gain or loss remains to be carried out. Yet, the following conclusions can be made.

General

- Change in state variables for both air-only and droplet-laden flow of low or high humidity can be described using a combination of isentropic and Rayleigh flow. That reveals a contrary influence of heat sinks through evaporation and heat sources through condensation. The systems loss is then determined by both decreased shock losses through heat addition, acceleration due to evaporation and momentum transfer from flow to droplets which directly impacts wake shape.

Air-only flow

- Loss coefficient is highest at dry conditions over the entire range of measured data, whereas humidity in general reduces the loss coefficient. The reason for this is a reduction of shock losses resulting in a smaller and less decelerated wake. As a result loss is reduced by 25 % at high and intermediate loading and X_L = 11 g/kg and about 30 % at low blade loading and X_L = 6 g/kg

- The swap in the maximum loss from high to intermediate humidity at low blade loading originates from the downward shifted shock position. High post shock Mach numbers at high humidity cannot be levelled and impact the mean flow velocity $\overline{w_2}$

- Deflection is reduced between 5 % and 15 % whereas deceleration ratio is altered only between 1 % and 4 %. Both effects are favourable for the overall loss reduction. However a lower deflection decreases the mere cascade performance output as well.

Droplet-laden flow

- The loss is dominated by increased momentum loss due to a thicker boundary on the suction side which is larger than the reduction in shock loss. Thus, the loss increases and is approximately 30 % higher for inflow angles $\beta_1 > 150°$. That increase gradually shrinks with smaller inflow angles to about 10 % at $\beta_1 > 146°$.

- The maximum isentropic Mach number is higher compared to air-only flow since droplets evaporate and accelerate the flow. Humid air is less accelerated because the amount of evaporation is limited by the saturation level. However, the effect of condensation is still observable when comparing pre shock Mach numbers at different humidities.

Two different goals have been issued during the research presented. The first adopts a promising description of compressible gas flow, including condensation and reviews it in the vicinity of a discrete fluid phase. The second concerns the impact of condensation on two-phase flow compressor cascade performance. Experiments reveal that for air-only flow ambient humidity has to be considered in the design process, particularly during numerical simulations. The condensation potential strongly alters the shock position and is favourable concerning losses, but reduces compressor stage's key parameters such as deflection. As for droplet-laden flows favourable humidity effects are decreased and may be neglected since the major loss arises from the increased boundary layer thickness with respect to the loss coefficient. However, a direct measurement of pressure based performance was not possible at the time. Last, published experimental data on that topic are rare so that data gathered herein may be of value to fellow researchers.

REFERENCES

[1] L. Balling. Fast cycling and rapid start-up: Newgeneration of plants achieves impressive results. *Modern Power Systems*, (1), 2011.

[2] G. H. Schnerr and U. Dohrmann. Drag and lift in nonadiabatic transonic flow. *AIAA Journal*, 32(1):101–107, 1994.

[3] G. H. Schnerr and U. Dohrmann. Transonic flow around airfoils with relaxation and energy supply by homogeneous condensation. *20th Fluid Dynamics, Plasma Dynamics and Lasers Conference*, 28(7):1187–1193, 1989.

[4] Y. Sasao and S. Yamamoto. Numerical Prediction of Humid Effect to Transonic Flows in Turbomachinery. *Proceedings of the International Gas Turbine Congress*, (IGTC2003 TS-021), 2003.

[5] T. Nagayama, Y. Kuramoto, and M. Imaizumi. The Effect of the Air Humidity on the Cascade Performance in the Suction Type Shock Tunnel. *Journal of the Japan Society for Aeronautical and Space Sciences*, 30(337), 1982.

[6] B. Ober. *Experimental Investigation on the Aerodynamic Performance of a Compressor Cascade in Droplet Laden Flow*. PhD thesis, Helmut-Schmidt-Universität, Hamburg, 10 2013.

[7] T. Eisfeld and F. Joos. New Boundary Layer Treatement Methods for Compressor Cascades. *8th Europ. Conf. Of Turbomachinery*, (ETC 23-27), 2009.

[8] N. Neupert, B. Ober, and F. Joos. Experimental Investigation on Droplet Behavior in a Transonic Compressor Cascade. *Journal of Turbomachinery*, 137(3), 2014.

[9] N. Neupert and F. Joos. Investigation on Water Film Induced Profile Losses in a Compressor Cascade. *Proceedings of ASME TurboExpo*, (GT2015-42153), 2015.

[10] N. Scholz. Über die Durchführung systematischer Messungen an ebenen Schaufelgittern. *Zeitschrift für Flugwissenschaften*, (10), 1956.

[11] N. Neupert. *Experimentelle Untersuchung einer tropfenbeladenen Strömung in einer ebenen Verdichterkaskade*. PhD thesis, Helmut-Schmidt-Universität, Hamburg, 05 2017.

[12] G. H. Schnerr. Unsteadiness in Condensing Flow: Dynamics of Internal Flows with Phase Transition and Application to Turbomachinery. *Proceedings of the Institution of Mechanical Engineers, Part C: Journal of Mechanical Engineering Science*, 219(12):1369–1410, 2005.

[13] C. E. Brennen. *Fundamentals of multiphase flow*. Cambridge University Press, Cambridge [England], New York, 2005.